

## RESEARCH PAPER

# Multimodal MRI as a diagnostic biomarker for amyotrophic lateral sclerosis

Bradley R. Foerster<sup>1,2,3</sup>, Ruth C. Carlos<sup>2</sup>, Ben A. Dwamena<sup>2,3</sup>, Brian C. Callaghan<sup>4</sup>, Myria Petrou<sup>1,2</sup>, Richard A. E. Edden<sup>1,5</sup>, Mona A. Mohamed<sup>1,5</sup>, Robert C. Welsh<sup>2,6</sup>, Peter B. Barker<sup>1,5</sup>, Eva L. Feldman<sup>4</sup> & Martin G. Pomper<sup>1</sup>

<sup>1</sup>Russell H. Morgan Department of Radiology and Radiological Science, Johns Hopkins University School of Medicine, Baltimore, Maryland

<sup>2</sup>Department of Radiology, University of Michigan, Ann Arbor, Michigan

<sup>3</sup>Ann Arbor VA Healthcare System, Ann Arbor, Michigan

<sup>4</sup>Department of Neurology, University of Michigan, Ann Arbor, Michigan

<sup>5</sup>F.M. Kirby Research Center for Functional Brain Imaging, Kennedy Krieger Institute, Baltimore, Maryland

<sup>6</sup>Department of Psychiatry, University of Michigan, Ann Arbor, Michigan

## Correspondence

Bradley R. Foerster, Department of Radiology, University of Michigan, 1500 E. Medical Center Drive, UH B2 A205H, Ann Arbor, MI 48109-5030. Tel: 1-734-615-3586; Fax: 1-734-764-2412; E-mail: compfun@umich.edu

## Funding Information

This study was funded by the A. Alfred Taubman Medical Research Institute.

Received: 8 November 2013; Revised: 16 December 2013; Accepted: 17 December 2013

*Annals of Clinical and Translational Neurology* 2014; 1(2): 107–114

doi: 10.1002/acn3.30

## Abstract

**Objective:** Reliable biomarkers for amyotrophic lateral sclerosis (ALS) are needed, given the clinical heterogeneity of the disease. Here, we provide proof-of-concept for using multimodal magnetic resonance imaging (MRI) as a diagnostic biomarker for ALS. Specifically, we evaluated the added diagnostic utility of proton magnetic resonance spectroscopy (MRS) to diffusion tensor imaging (DTI). **Methods:** Twenty-nine patients with ALS and 30 age- and gender-matched healthy controls underwent brain MRI which used proton MRS including spectral editing techniques to measure  $\gamma$ -aminobutyric acid (GABA) and DTI to measure fractional anisotropy of the corticospinal tract. Data were analyzed using logistic regression, *t*-tests, and generalized linear models with leave-one-out analysis to generate and compare the resulting receiver operating characteristic (ROC) curves. **Results:** The diagnostic accuracy is significantly improved when the MRS data were combined with the DTI data as compared to the DTI data only (area under the ROC curves (AUC) = 0.93 vs. AUC = 0.81; *P* = 0.05). The combined MRS and DTI data resulted in sensitivity of 0.93, specificity of 0.85, positive likelihood ratio of 6.20, and negative likelihood ratio of 0.08 whereas the DTI data only resulted in sensitivity of 0.86, specificity of 0.70, positive likelihood ratio of 2.87, and negative likelihood ratio of 0.20. **Interpretation:** Combining multiple advanced neuroimaging modalities significantly improves disease discrimination between ALS patients and healthy controls. These results provide an important step toward advancing a multimodal MRI approach along the diagnostic test development pathway for ALS.

## Introduction

Amyotrophic lateral sclerosis (ALS) is a degenerative motor neuron disease involving upper and lower motor neurons (LMN). The disease has a uniformly fatal outcome with median survival times of 2–4 years.<sup>1</sup> ALS can be a challenging disease to diagnose and provide prognostic information at an individual level given its heterogeneous clinical presentation and lack of definitive tests. Diagnosis of ALS is based on clinical history and examination, and relies on the detection of upper and LMN

signs in multiple body segments.<sup>2</sup> These factors contribute to a nearly 1-year delay on average from the initial symptom onset to diagnosis with a delayed diagnosis of 4 months even after been seen by a neurologist.<sup>3,4</sup> Furthermore, over 40% of ALS patients undergo incorrect medical treatment including surgical intervention.<sup>5</sup> Reliable biomarkers for ALS are needed both for diagnostic as well as prognostic purposes.<sup>6,7</sup>

Electromyography (EMG) supplements the clinical evaluation of LMN pathology in ALS and can detect signs of LMN denervation in muscles that appear normal on

physical examination.<sup>8</sup> Conventional neuroimaging techniques that evaluate structural changes lack the specificity and sensitivity to serve as an “EMG” surrogate of upper motor neuron (UMN) involvement for ALS and detect clinically occult UMN signs.<sup>9–11</sup> As a result, the main purpose of conventional magnetic resonance imaging (MRI) techniques is to rule out alternative diagnoses that may mimic ALS such as upper cervical cord lesions, which can produce both UMN and LMN neurological signs. Therefore, great interest exists in using advanced neuroimaging methods such as diffusion tensor imaging (DTI) and magnetic resonance spectroscopy (MRS) to develop accurate diagnostic biomarkers for ALS. DTI allows for in vivo measurement and quantification of water movement, which has been demonstrated to be altered in ALS, providing evidence of damaged white matter tracts.<sup>7</sup> MRS allows for in vivo measurement of brain metabolites. Using MRS in ALS patients, *N*-acetylaspartate (NAA), a marker of neuronal integrity, has been shown to be decreased in the motor cortex (MC), and myo-inositol (mI), a marker of glial cells, has been shown to be increased in the MC.<sup>12</sup> A potential additional diagnostic biomarker is  $\gamma$ -aminobutyric acid (GABA), the major inhibitory neurotransmitter in the central nervous system. There is increasing evidence that reduced inhibitory function may play an important role in the pathogenesis of ALS.<sup>13</sup> We have recently published two MRS studies that used spectral editing techniques to demonstrate a decrease in GABA in ALS patients.<sup>14,15</sup>

We are interested in systematically evaluating the potential of advanced imaging methods to serve as a biomarker in ALS. As an initial step, we have performed two meta-analysis studies indicating that DTI by itself currently lacks sufficient diagnostic discrimination to be implemented in the clinical setting.<sup>16,17</sup> We concluded that additional diagnostic tests will have to be combined with DTI to develop a clinically relevant testing algorithm. As a next step in diagnostic test development, we have conducted a “Phase 2a” trial which combines MRS and DTI to compare ALS patients with well-established disease to healthy controls (HC) as a proof-of-concept.<sup>18</sup> The aim of this study is to explore the added diagnostic utility of MRS, including spectral editing techniques that enable quantification of GABA, to DTI in the setting of ALS.

## Subjects/Materials and Methods

Twenty-nine right-handed ALS patients and 30 age- and gender-matched right-handed HCs were recruited. Our institutional review board approved all study protocols, and informed written consent was obtained from all of the participants. Subjects were excluded if they had a his-

tory of head injury, cerebrovascular disease, central nervous system infection, active substance abuse, or contraindication for MRI. ALS patients were classified by experienced ALS neurologists (B.C.C., E.L.F.) as definite ( $n = 4$ ), probable ( $n = 15$ ), or probable laboratory supported ( $n = 10$ ) according to the revised El Escorial Criteria.<sup>2</sup> In addition, the ALS patients were examined (B.C.C., E.L.F.) for presence of muscle spasticity and pathologic reflexes in the different body segments. The Ashworth Spasticity Scale (range 0–8),<sup>19</sup> presence of pathological reflexes (range 0–24),<sup>20,21</sup> and the Center for Neurologic Study – Lability Scale for pseudobulbar affect (range 0–1)<sup>22</sup> were used to measure UMN disease involvement resulting in a range of 0–33 with a higher score reflecting greater disease burden. The MRI study was performed within 2 months of the neurological exam. Seven of the ALS patients had bulbar-onset disease and 22 patients had limb-onset disease. Fifteen of the ALS patients were on riluzole treatment for ALS and 14 of the ALS patients were riluzole treatment-naïve. Participant characteristics are summarized in Table 1.

## Diffusion tensor imaging

Nineteen subjects (10 ALS, 9 HCs) were imaged on a Philips Achieva 3T system (Best, Netherlands) using an 8-channel receive head coil. Forty subjects (19 ALS, 21 HCs) were imaged on a Philips Ingenia 3T system (Best, Netherlands) using a 15-channel receive head coil. Whole brain diffusion-weighted imaging was obtained using a multiple shot spin-echo technique (repetition time/echo time = 7075/62 msec, field of view 112 mm, 2-mm isotropic resolution,  $b$  values = 0, 800 sec/mm<sup>2</sup>, 15 isotropically distributed gradients). ExploreDTI v4.8.2 (Utrecht, the Netherlands) was used to perform the data processing with incorporating a motion and eddy current correction

**Table 1.** Participant characteristics.

	Controls	ALS
No.	30	29
Age, year, mean $\pm$ SD (range)	59.3 $\pm$ 9.9 (29–79)	59.5 $\pm$ 10.2 (32–78)
Male:female	20:10	17:12
Disease duration, month, mean $\pm$ SD (range)	NA	28.6 $\pm$ 14.5 (4–64)
UMN Score, mean $\pm$ SD (range)	NA	15.6 $\pm$ 7.0 (1–27)
ALSFRS-R Score, mean $\pm$ SD (range)	NA	34.1 $\pm$ 8.2 (18–47)

ALS, amyotrophic lateral sclerosis; ALSFRS-R, revised Amyotrophic Lateral Sclerosis Functional Rating Scale, UMN, upper motor neuron.

algorithm. Seed regions of interest were placed in the posterior limb of the internal capsule and pons using detailed white matter atlases to generate the fiber tracks using standard deterministic stream.<sup>23</sup> The fractional anisotropy (FA) values for the right and left corticospinal tract were calculated and averaged. Figure 1 depicts the fiber tracking of the corticospinal tracts as well as the MRS voxel placement in the left MC and resulting spectra.

### Magnetic resonance spectroscopy

The MRS results from this cohort have been previously published.<sup>14,15</sup> T<sub>1</sub>-weighted 3D-MPRAGE images were used to specify the placement of a 3.0 × 3.0 × 2.0 cm voxel in the left MC manually centered on the hand knob in the axial projection and the hook in the sagittal projection under supervision of an experienced neuroradiologist (B.R.F.).<sup>24</sup> Single-voxel point resolved spectroscopy (PRESS) and Mescher-Garwood point resolved spectroscopy (MEGA-PRESS) data acquisitions were performed.<sup>25</sup> PRESS spectra (TR/TE = 2000/35 msec) were acquired using “VAPOR” water suppression with 32 averages acquired. LCModel (version 6.1-4A; S. Provencher, Ph.D., Oakville, Ontario, Canada)<sup>26</sup> was used to analyze the PRESS data. In order to be used in the analysis, the Cramér-Rao lower bounds as generated in LCModel for the metabolites needed to be less than 20%. MEGA-PRESS spectra were acquired using TE = 68 msec (TE<sub>1</sub> = 15 msec, TE<sub>2</sub> = 53 msec); TR = 1.8 sec; 256 averages; frequency selective editing pulses (14 msec) applied at 1.9 ppm (ON) and 7.46 ppm (OFF). Gaussian curve fits were generated of the GABA and inverted NAA peaks using in-house post processing software in Matlab 2012a (Mathworks, Natick, MA) and the GABA levels were calculated relative to the NAA signal in the edited spectra.<sup>27</sup> The NAA concentration generated from the LCModel analysis of the short-TE PRESS spectrum was then multiplied by the GABA/NAA ratio to provide an estimate of GABA concentration. SPM5 (Wellcome Trust Centre for Neuroimaging, London, England) was used to segment the voxels into gray matter, white matter, and cerebrospinal fluid percentages. Imaging analyses for both DTI and MRS measures were performed with the disease status of the subject blinded.

### Statistical analyses

Stata v.11 (StataCorp, College Station, TX) was used for the statistical analysis. Using scanner type (Achieva or Ingenia) as a covariate, logistic regression analyses were performed between disease status and individual FA and metabolite values. Distribution of the data was evaluated using the Shapiro-Wilk test. Differences in FA and brain metabolite values were determined using two-tailed inde-

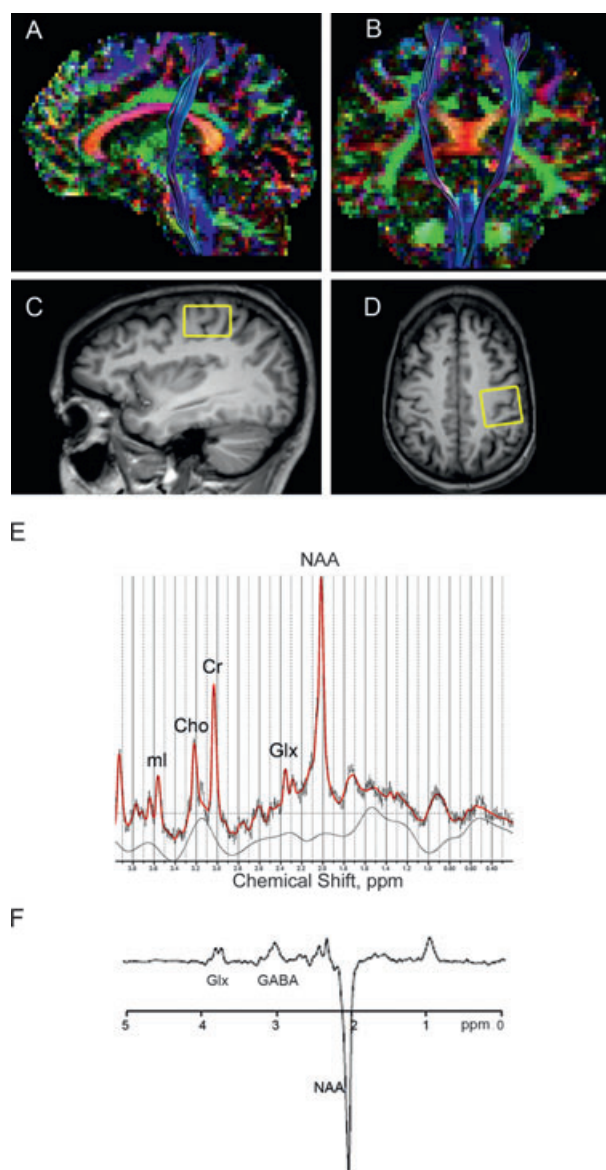


**Figure 1.** Diffusion tractography and voxel placement with resulting magnetic resonance spectra. Images showing diffusion tractography of the corticospinal tract in the sagittal (A) and coronal projections (B). Voxel placement for magnetic resonance spectroscopy of the motor cortex region in the sagittal (C) and axial (D) projections (F). Representative magnetic resonance spectroscopy spectrum from the motor cortex of an ALS subject using PRESS (E) and MEGA-PRESS editing technique (F).

pendent sample *t*-test between ALS patients and HCs. A post hoc analysis was performed comparing gray matter and white matter percentages after normalizing to cerebrospinal fluid percentage between ALS patients and HCs using an independent sample *t*-test. Associations between the MRI measures (MRS and DTI) and clinical status (revised Amyotrophic Lateral Sclerosis Functional Rating

Scale [ALSFRS-R], disease duration, average UMN score and contralateral UMN score) were performed using Pearson correlations. The generalized linear model command in Stata, `incroc`, was used to generate and compare the receiver operating characteristic (ROC) curves and the area under the ROC curves (AUC) for the different models using leave-one-out cross-validation analysis and bootstrapping. The two models were (1) DTI FA alone (Model 1), and (2) DTI FA + MRS NAA + MRS mI + MRS GABA (Model 2). Scanner type was also included as a categorical variable in each model. The optimal cut point to generate the sensitivity and specificity was determined using the Youden index, which places equal weight to sensitivity and specificity measures.

## Results

### Group level imaging measures

DTI FA data and conventional MRS data were obtained from all subjects. For the MEGA-PRESS acquisition, GABA spectra in the MC of two ALS patients and one HC had inadequate signal-to-noise ratio. There were no significant effects of MRI scanner type for the MRS or DTI FA values ( $Z > 0.05$  for all). There were no significant differences between gray matter and white matter percentages between the ALS patients and HCs ( $P > 0.05$ ). The data for the MRS and DTI FA were normally distributed ( $P > 0.05$  for all).

FA levels were lower in ALS patients (mean  $\pm$  SD  $0.534 \pm 0.028$ ) compared to HCs ( $0.569 \pm 0.022$ ;  $P < 0.001$ ). NAA levels in the left MC were lower in ALS patients ( $7.70 \pm 0.83$  IU) compared to HCs ( $8.20 \pm$

$0.49$  IU;  $P = 0.008$ ). Myo-inositol levels in the left MC were higher in ALS patients ( $3.71 \pm 0.67$  IU) compared to HCs ( $3.14 \pm 0.43$  IU;  $P < 0.001$ ). GABA levels in the MC were lower in ALS patients ( $1.45 \pm 0.30$  IU) compared to HCs ( $1.72 \pm 0.34$  IU;  $P = 0.002$ ). Results are presented in Figure 2.

Riluzole treatment subanalyses showed that there were significantly higher NAA levels and FA levels in riluzole-naïve patients with ALS compared to riluzole-treated patients with ALS ( $P = 0.007$  and  $P = 0.03$ , respectively). There were no significant differences in mI levels or GABA levels between the riluzole-naïve patients with ALS and riluzole-treated patients with ALS. There were significant correlations between the MC GABA and disease duration ( $r = -0.39$ ,  $P = 0.05$ ), MC NAA and ALSFRS-R score ( $r = 0.39$ ,  $P < 0.05$ ), DTI FA and ALSFRS-R score ( $r = 0.46$ ,  $P < 0.05$ ).

### ROC and AUC

Figure 3 shows the ROC curve for DTI FA (Model 1) and DTI FA + MRS NAA + MRS mI + MRS GABA (Model 2). The AUC for Model 1 was 0.81 (95% CI: 0.70–0.93) and the AUC for Model 2 was significantly higher with a value of 0.93 (95% CI: 0.87–0.99;  $P = 0.05$ ). Scanner type was not a significant covariate in Model 1 ( $P > 0.05$ ) or Model 2 ( $P > 0.05$ ).

### Sensitivity, specificity, and predictive values

Sensitivity and specificity of Model 1 were 0.86 and 0.70, respectively. Sensitivity and specificity of Model 2 were 0.93 and 0.85, respectively. For Model 1, the positive

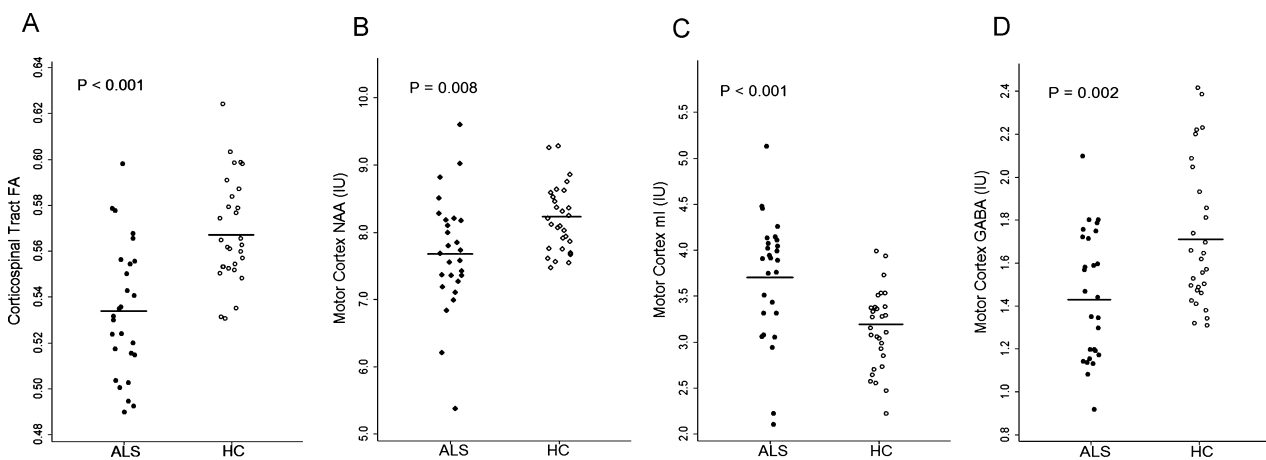


**Figure 2.** Decreased fractional anisotropy (FA), decreased N-acetylaspartate (NAA), increased myo-inositol (mI), and decreased  $\gamma$ -aminobutyric acid (GABA) levels in amyotrophic lateral sclerosis (ALS) patients. Circles represent respective values of FA in the corticospinal tract (A), NAA in the left motor cortex (B), mI in the left motor cortex (C), and GABA levels in the left motor cortex (D) for individual ALS patients and healthy controls (HC). Horizontal bars indicate the mean. IU, institutional units.

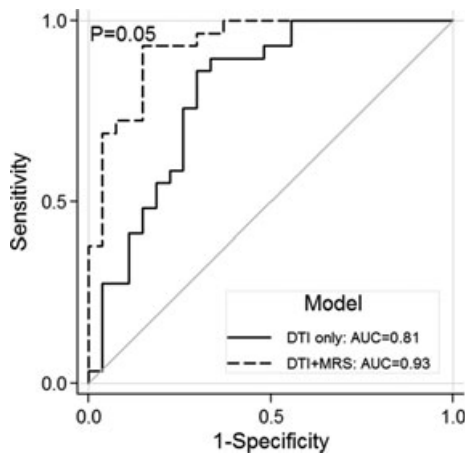


**Figure 3.** Significant increase in diagnostic accuracy combining magnetic resonance spectroscopy (MRS) and diffusion tensor imaging (DTI) measures. Receiver operating characteristic (ROC) curves comparing DTI diagnostic test accuracy model to combined DTI and MRS model. Solid ROC curve represents the model using DTI fractional anisotropy values. Dashed ROC curve represents the model using DTI fractional anisotropy, MRS N-acetylaspartate, MRS myo-inositol, and MRS  $\gamma$ -aminobutyric acid values combined.

likelihood ratio was 2.87 and the negative likelihood ratio was 0.20. For Model 2, the positive likelihood ratio was 6.20 and the negative likelihood ratio was 0.08. Using Bayesian methods, the posttest probabilities of disease after negative and positive test results using different

disease pretest probabilities for the two models are presented in Figure 4.

### Discussion

By combining MRS measures with DTI FA values, we demonstrate a statistically significant improvement in the diagnostic accuracy in distinguishing between ALS patients with well-established disease and HCs, with a relatively high AUC value of 0.93. Furthermore, the combination of MRS and DTI measures results in improved positive and negative likelihood ratios. These findings support addition of relevant metabolite concentrations from MRS to FA values derived from DTI, so that together these MRI-generated parameters can provide a potentially useful noninvasive biomarker for ALS.

The posttest probability graph helps to place our results in clinical context (Fig. 4). For an individual with an ALS pretest probability of 0.50, the posttest probability of ALS is 0.74 using the DTI FA measure only and 0.86 when combining DTI and MRS measures with a positive test result. Using the same pretest probability of 0.50, the posttest probability of ALS is 0.17 using the DTI FA measure only and 0.08 when combining DTI and MRS measures with a negative test result. We chose to use the Youden index rather than the point on the ROC curve closest to (0, 1), as the Youden index has been shown to maximize the overall correct classification rate.<sup>28</sup> It is

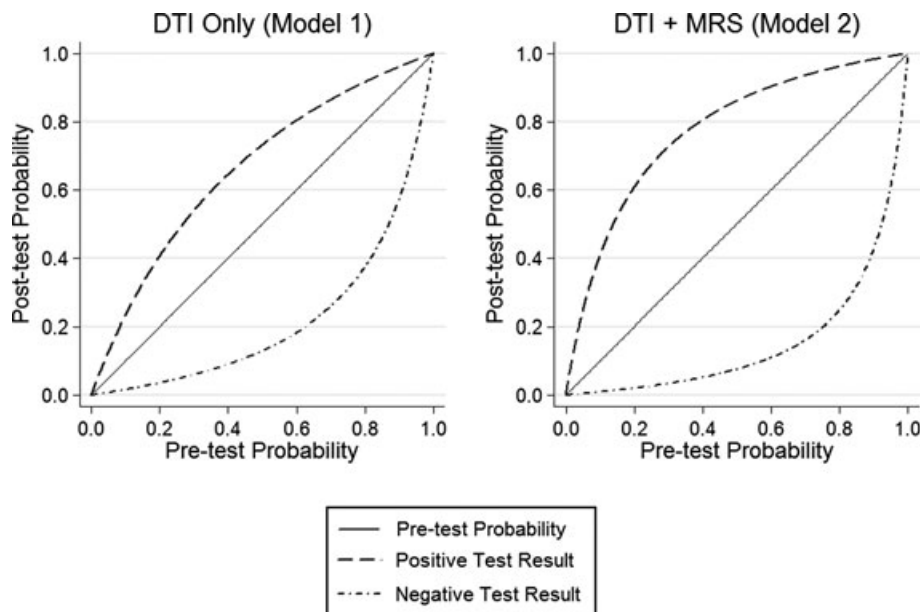


**Figure 4.** Posttest probabilities using diffusion tensor imaging (DTI) only and diffusion tensor imaging combined with magnetic resonance spectroscopy (MRS). Posttest probabilities for imaging results for each of the two models using hypothetical populations with different pretest disease probabilities. Model 1 used the DTI fractional anisotropy values only. Model 2 uses the DTI fractional anisotropy combined with MRS N-acetylaspartate, MRS myo-inositol and MRS  $\gamma$ -aminobutyric acid values.

important to mention that leave-one-out cross-validation statistical analysis was implemented to avoid overfitting of the model and subsequent overestimation of diagnostic accuracy.

A large number of DTI and MRS studies have been performed that have investigated differences in DTI measures and brain metabolites in the setting of ALS including a number of studies that have included both DTI and MRS acquisitions.<sup>29–33</sup> Although a few of these studies have evaluated the potential diagnostic utility of either DTI or MRS,<sup>32,33</sup> the combination of these two advanced neuroimaging techniques for diagnostic accuracy has not been investigated. There have been recent ALS publications that have combined DTI with other advanced MR techniques including resting state fMRI<sup>34</sup> and voxel-based morphometry measures<sup>35</sup> with encouraging disease discrimination results. Combining multiple MRI methods to improve disease classification has also been applied in other neurodegenerative diseases. For example, a multivariate analysis approach has been applied to Alzheimer's disease using a combination of MRS and MRI volumetric metrics to increase diagnostic accuracy and resulted in a sensitivity of 0.97 and a specificity of 0.94.<sup>36</sup>

We focused our MRS measures to include NAA, a measure of neuronal integrity, mI, a glial cell marker, and GABA, the major inhibitory neurotransmitter in the central nervous system, based on the significant differences between ALS patients and HCs. Our findings of decreased NAA and increased mI are in accord with other published studies.<sup>37–40</sup> Our findings of reduced GABA levels in the MC are supported by other indirect evidence of decreased cortical inhibition in ALS, including an ALS animal model, as well as human histochemical, positron emission tomography, and transcranial magnetic stimulation studies.<sup>41–44</sup> For the DTI measures, we chose to focus on FA as this is the most commonly altered DTI measure in the ALS literature.<sup>16</sup>

This study constitutes a critical early step in the development and evaluation of diagnostic testing, in this case a multimodal MRI approach for the evaluation of ALS patients. In this study, we are establishing the performance of our testing algorithm to differentiate between patients with well-established disease compared to HC subjects. The effectiveness of the diagnostic testing algorithm among these cohorts lays the groundwork for the subsequent phases of diagnostic test development and validation which include incorporating diseased subjects with varying severity of disease (Phase 2b) as well as subjects who are only suspected of having the disease (Phase 2c).<sup>18,45</sup>

As in most ALS imaging studies, our cohort predominantly consisted of patients with later stage disease, which could accentuate effect sizes of the DTI and MRS altera-

tions, specifically the observed changes in mI.<sup>46</sup> Nevertheless, this approach is important in the proof-of-concept stage. This study represents an early, but necessary, evaluation of a new diagnostic algorithm according to the standard methodology of technology assessment over its lifespan. This imaging study uses one of the larger cohorts of ALS patients reported to date. However, future diagnostic evaluation studies using multimodal MRI will benefit from including ALS patients with earlier disease stages as well as a wider spectrum of disease, to decrease spectrum bias. Longitudinal studies in patients with suspected ALS, based on clinical and functional markers, using the proposed imaging algorithm will need to be conducted to determine the sensitivity of the algorithm to changes in clinical and functional status and to assess rate of disease conversion to definite ALS. If information from these more extensive studies suggests a correlation between imaging measures and disease severity, the potential of multimodal MR imaging as a prognostic marker can be also evaluated in a longitudinal setting.

Limitations of this study include the potential contributions from macromolecules with similar coupling properties to the GABA signal at 3 ppm. Due to time considerations, this study only implemented 15-direction DTI acquisition that has been shown to add variability to the FA results compared to 20 or more direction DTI acquisitions.<sup>47</sup> A longitudinal trial enrolling ALS patients prior to initiation of therapy is required to assess the effect of riluzole treatment on the measured MRI metrics. We also did not include subjects with diseases that can mimic ALS, such as multifocal motor neuropathy, which would be helpful in validating the specificity of the MRS and DTI metrics.

In conclusion, adding MRS measures to DTI FA measures leads to significantly increased diagnostic accuracy in distinguishing ALS patients with well-established disease from HCs. This corresponds to a successful Phase 2a trial in the established algorithm of diagnostic test development. As such, this provides the foundation for Phase 2b and 2c trials, that is, assessing whether the combined MRS-DTI measures are related to severity of disease and evaluating test accuracy performance in subjects with suspected disease. Additional research efforts and multicenter diagnostic trial evaluations are needed to optimize imaging protocols, validate diagnostic accuracy across a clinically representative disease spectrum, and to understand whether these techniques can discriminate between ALS and diseases that mimic ALS.

## Acknowledgments

This study was funded by the A. Alfred Taubman Medical Research Institute. The authors thank MR senior research

technologist Suzan Lowe for her assistance in imaging data acquisition. Carlos has served as a consultant for Philips Healthcare. Barker is a consultant for Olea Medical, Marseille, France. The authors have no other relationships that might lead to a perceived conflict of interest.

## Conflict of Interest

None declared.

## References

- Eisen A, Schulzer M, MacNeil M, et al. Duration of amyotrophic lateral sclerosis is age dependent. *Muscle Nerve* 1993;16:27–32.
- Brooks BR, Miller RG, Swash M, Munsat TL. El Escorial revisited: revised criteria for the diagnosis of amyotrophic lateral sclerosis. *Amyotroph Lateral Scler Other Motor Neuron Disord* 2000;1:293–299.
- Zoccollella S, Beghi E, Palagano G, et al. Predictors of delay in the diagnosis and clinical trial entry of amyotrophic lateral sclerosis patients: a population-based study. *J Neurol Sci* 2006;250:45–49.
- Househam E, Swash M. Diagnostic delay in amyotrophic lateral sclerosis: what scope for improvement? *J Neurol Sci* 2000;180:76–81.
- Kraemer M, Buerger M, Berlit P. Diagnostic problems and delay of diagnosis in amyotrophic lateral sclerosis. *Clin Neurol Neurosurg* 2010;112:103–105.
- Turner MR, Kiernan MC, Leigh PN, Talbot K. Biomarkers in amyotrophic lateral sclerosis. *Lancet Neurol* 2009;8: 94–109.
- Bowser R, Turner MR, Shefner J. Biomarkers in amyotrophic lateral sclerosis: opportunities and limitations. *Nat Rev Neurol* 2011;7:631–638.
- Eisen A, Swash M. Clinical neurophysiology of ALS. *Clin Neurophysiol* 2001;112:2190–2201.
- Cheung G, Gawel MJ, Cooper PW, et al. Amyotrophic lateral sclerosis: correlation of clinical and MR imaging findings. *Radiology* 1995;194:263–270.
- Comi G, Rovaris M, Leocani L. Review neuroimaging in amyotrophic lateral sclerosis. *Eur J Neurol* 1999;6:629–637.
- Hofmann E, Ochs G, Pelzl A, Warmuth-Metz M. The corticospinal tract in amyotrophic lateral sclerosis: an MRI study. *Neuroradiology* 1998;40:71–75.
- Turner MR, Agosta F, Bede P, et al. Neuroimaging in amyotrophic lateral sclerosis. *Biomark Med* 2012;6:319–337.
- Turner MR, Kiernan MC. Does interneuronal dysfunction contribute to neurodegeneration in amyotrophic lateral sclerosis? *Amyotroph Lateral Scler* 2012;13:245–250.
- Foerster BR, Callaghan BC, Petrou M, et al. Decreased motor cortex gamma-aminobutyric acid in amyotrophic lateral sclerosis. *Neurology* 2012;78:1596–1600.
- Foerster BR, Pomper MG, Callaghan BC, et al. An imbalance between excitatory and inhibitory neurotransmitters in amyotrophic lateral sclerosis revealed by use of 3-T proton magnetic resonance spectroscopy. *JAMA Neurol* 2013;24:1–8.
- Foerster BR, Dwamena BA, Petrou M, et al. Diagnostic accuracy using diffusion tensor imaging in the diagnosis of ALS: a meta-analysis. *Acad Radiol* 2012;19:1075–1086.
- Foerster BR, Dwamena BA, Petrou M, et al. Diagnostic accuracy of diffusion tensor imaging in amyotrophic lateral sclerosis: a systematic review and individual patient data meta-analysis. *Acad Radiol* 2013;20: 1099–1106.
- Gluud C, Gluud LL. Evidence based diagnostics. *BMJ* 2005;330:724–726.
- Bohannon RW, Smith MB. Interrater reliability of a modified Ashworth scale of muscle spasticity. *Phys Ther* 1987;67:206–207.
- Turner MR, Cagnin A, Turkheimer FE, et al. Evidence of widespread cerebral microglial activation in amyotrophic lateral sclerosis: an [11C](R)-PK11195 positron emission tomography study. *Neurobiol Dis* 2004;15: 601–609.
- Ellis CM, Simmons A, Jones DK, et al. Diffusion tensor MRI assesses corticospinal tract damage in ALS. *Neurology* 1999;53:1051–1058.
- Moore SR, Gresham LS, Bromberg MB, et al. A self report measure of affective lability. *J Neurol Neurosurg Psychiatry* 1997;63:89–93.
- Mori S, Wakana, S, Van Zijl PCM. MRI atlas of human white matter. 1st ed. Amsterdam, The Netherlands; San Diego, CA: Elsevier, 2004.
- Yousry TA, Schmid UD, Alkadhi H, et al. Localization of the motor hand area to a knob on the precentral gyrus. A new landmark. *Brain* 1997;120(Pt 1):141–157.
- Mescher M, Merkle H, Kirsch J, et al. Simultaneous in vivo spectral editing and water suppression. *NMR Biomed* 1998;11:266–272.
- Provencher SW. Estimation of metabolite concentrations from localized in vivo proton NMR spectra. *Magn Reson Med* 1993;30:672–679.
- Stagg CJ, Best JG, Stephenson MC, et al. Polarity-sensitive modulation of cortical neurotransmitters by transcranial stimulation. *J Neurosci* 2009;29:5202–5206.
- Perkins NJ, Schisterman EF. The inconsistency of “optimal” cutpoints obtained using two criteria based on the receiver operating characteristic curve. *Am J Epidemiol* 2006;163:670–675.
- Wang S, Poptani H, Woo JH, et al. Amyotrophic lateral sclerosis: diffusion-tensor and chemical shift MR imaging at 3.0 T. *Radiology* 2006;239:831–838.
- Mitsumoto H, Ulug AM, Pullman SL, et al. Quantitative objective markers for upper and lower motor neuron dysfunction in ALS. *Neurology* 2007;68:1402–1410.
- Nelles M, Block W, Traber F, et al. Combined 3T diffusion tensor tractography and 1H-MR spectroscopy in

- motor neuron disease. *AJNR Am J Neuroradiol* 2008;29:1708–1714.
32. Pyra T, Hui B, Hanstock C, et al. Combined structural and neurochemical evaluation of the corticospinal tract in amyotrophic lateral sclerosis. *Amyotroph Lateral Scler* 2010;11:157–165.
  33. Lombardo F, Frijia F, Bongioanni P, et al. Diffusion tensor MRI and MR spectroscopy in long lasting upper motor neuron involvement in amyotrophic lateral sclerosis. *Arch Ital Biol* 2009;147:69–82.
  34. Douaud G, Filippini N, Knight S, et al. Integration of structural and functional magnetic resonance imaging in amyotrophic lateral sclerosis. *Brain* 2011;134(Pt 12):3470–3479.
  35. Filippini N, Douaud G, Mackay CE, et al. Corpus callosum involvement is a consistent feature of amyotrophic lateral sclerosis. *Neurology* 2010;75:1645–1652.
  36. Westman E, Wahlund LO, Foy C, et al. Magnetic resonance imaging and magnetic resonance spectroscopy for detection of early Alzheimer's disease. *J Alzheimers Dis* 2011;26(Suppl. 3):307–319.
  37. Agosta F, Chio A, Cosottini M, et al. The present and the future of neuroimaging in amyotrophic lateral sclerosis. *AJNR Am J Neuroradiol* 2010;31:1769–1777.
  38. Block W, Karitzky J, Traber F, et al. Proton magnetic resonance spectroscopy of the primary motor cortex in patients with motor neuron disease: subgroup analysis and follow-up measurements. *Arch Neurol* 1998;55:931–936.
  39. Bowen BC, Pattany PM, Bradley WG, et al. MR imaging and localized proton spectroscopy of the precentral gyrus in amyotrophic lateral sclerosis. *AJNR Am J Neuroradiol* 2000;21:647–658.
  40. Kalra S, Hanstock CC, Martin WR, et al. Detection of cerebral degeneration in amyotrophic lateral sclerosis using high-field magnetic resonance spectroscopy. *Arch Neurol* 2006;63:1144–1148.
  41. Nieto-Gonzalez JL, Moser J, Lauritzen M, et al. Reduced GABAergic inhibition explains cortical hyperexcitability in the wobbler mouse model of ALS. *Cereb Cortex* 2011;21:625–635.
  42. Petri S, Krampfl K, Hashemi F, et al. Distribution of GABAA receptor mRNA in the motor cortex of ALS patients. *J Neuropathol Exp Neurol* 2003;62:1041–1051.
  43. Turner MR, Osei-Lah AD, Hammers A, et al. Abnormal cortical excitability in sporadic but not homozygous D90A SOD1 ALS. *J Neurol Neurosurg Psychiatry* 2005;76:1279–1285.
  44. Vucic S, Kiernan MC. Novel threshold tracking techniques suggest that cortical hyperexcitability is an early feature of motor neuron disease. *Brain* 2006;129(Pt 9):2436–2446.
  45. Sackett DL, Haynes RB. The architecture of diagnostic research. *BMJ* 2002;324:539–541.
  46. van der Graaff MM, Lavini C, Akkerman EM, et al. MR spectroscopy findings in early stages of motor neuron disease. *AJNR Am J Neuroradiol* 2010;31:1799–1806.
  47. Jones DK. The effect of gradient sampling schemes on measures derived from diffusion tensor MRI: a Monte Carlo study. *Magn Reson Med* 2004;51:807–815.